Folate-based *in vivo* reprogramming of dentate gyrus improves cognitive function in old mice

Antón-Fernández A[1]; Cuadros R[1,2]; Peinado-Cahuchola R[1]; Hernández F[1]; Avila J[1,2*]

[1] Centro de Biología Molecular "Severo Ochoa", CSIC/UAM, Universidad Autónoma de Madrid, Cantoblanco, 28049 Madrid, Spain.
[2] Center for Networked Biomedical Research on Neurodegenerative Diseases (CIBERNED), Madrid, Spain.

[*] Correspondence to: Jesús Avila, Centro de Biología Molecular "Severo Ochoa", CSIC/UAM, Universidad Autónoma de Madrid, Cantoblanco, 28049 Madrid, Spain. Electronic address: javila@cbm.csic.es.

Acknowledgements & Funding

We would like to acknowledge the comments, corrections and advice given by Prof. Carlos López-Otín. We thank Ms. Nuria de la Torre Alonso for technical and editorial assistance. We also thank the Optical and Confocal Microscopy Facility (SMOC) at CBMSO-CSIC for technical support. Scheme figure 7 created with Biorender (BioRender.com).
This work has been supported by grants from the Spanish Ministry of Economy and competitiveness: PGC-2018-09177-B-100 (J.A.), PID2020-113204GB-I00 (F.H.) and PID2021-123859OB-100 from MCIN /AEI/10.13039/501100011033 / FEDER, UE (J.A.). This work was supported by CSIC through an intramural grant (201920E104) (J.A.). The Centro de Biología Molecular Severo Ochoa (CBMSO) is a *Severo Ochoa* Center of Excellence (MICIN, award CEX2021-001154-S).

Abstract

Here we report a novel strategy to rejuvenate dentate gyrus cells in old mice. This approach involves the use of simple compounds such as folate and a peptide that binds to folate receptor α. The injection of folate or folate-mimicking peptide into the brain brought about a significant enhancement of cognition. Likewise, the dentate gyrus cells of these mice showed increased plasticity and DNA methylation levels. On the basis of our findings, we propose that folate, and folate-mimicking peptides acting on folate receptor α enhance neural plasticity in a similar fashion to the OSKM (Oct4, Sox2, Klf4, and Myc) Yamanaka factors. However, in marked contrast with the long-term cyclic treatment used for cell reprogramming with the latter, our method involves only a single injection of very simple small compounds. Our observations may facilitate future studies aimed at improving the clinical translation of cell reprogramming methods into the field of neurodegenerative disorders.

Keywords: Aging; Folate; Reprogramming; Cognition; Folate Receptor; Hippocampus

Introduction

Epigenetic changes are hallmark features of aging [25]. Indeed, organismal aging can be monitored by studying several epigenetic chromatin markers [41]. Given that aging-dependent epigenetic changes can be modified to younger levels, the reversion of some aging characteristics is feasible [3, 33, 61]. The erasure of aging-dependent epigenetic changes can be achived using the so-called Yamanaka Factors (YF) [44, 54], and the cyclic expression of these factors ameliorates the hallmarks of aging in peripheral tissues [8, 27, 39]. Indeed, a similar approach to that used for peripheral tissue, namely controlled cell reprogramming by cyclic expression of YF, causes an amelioration of the aging features in the dentate gyrus (DG) of old mice, thereby improving memory [36].

Given that YF are transcription factors [44], they can also alter transcription. Thus, epigenetic or transcriptional changes, or both, can occur when YF are expressed in old cells.

Here we tested a strategy to rejuvenate aging brain cells through specific reprogramming [7] but using small simple compounds [18] instead of YF. In this regard, YF may reprogram neurons in the brains of old mice through the following: a) an increase in adult hippocampal neurogenesis (AHN) [36]; b) epigenetic changes (methylation) in histones or DNA [32, 36]; or c) acting YF as transcription factors [59]. Thus, here we tested whether small compounds could replicate the effects of YF. Our findings showed that the compounds tested had no impact on AHN. It is known that YF control epigenetic changes like those related to the regulation of histone and DNA methylation [27, 36]. Changes in the latter sustain the development of the epigenetic clock, which may predict biological (chronological) age [17]. Histone and DNA methylation involves methyl donors, methyltransferases, and, sometimes, coenzymes like vitamin B12 [12]. The universal methyl-donor is methionine but other factors like folate could be involved indirectly [12]. It has been reported that YF and their related Thompson factors [32] increase the activity of DNA methyltransferases like the DNMT family [24, 48, 57]. Given that DNA methylation can increase in the presence of methyltransferases, through the presence of methyl-donors like the universal methyl-donor (methionine), folate, or cofactors like vitamin B12 [12], here we studied whether the presence of any of these small compounds could replicate the effects of YF in the amelioration of aging features in the dentate gyrus (DG) [36]. Our results suggest that the presence of folate is enough to achieve amelioration and also to induce changes in the degree of DNA methylation. Furthermore, folate could act on cells by binding to folate receptors, folate receptor α (FRα) being the most studied receptor, which, in addition, could serve as a transcriptional factor [5]. Here we tested the capacity of a synthetic FRα-binding peptide [20] to mimic folate as an inducer of FRα transcriptional function. Indeed, the brain injection of this peptide resulted in similar positive cognitive effects to those achieved with folate injections. Given these observations, this FRα-binding peptide emerges as a potential alternative to folate to improve cognition.

Materials and Methods

1. *Animals*

A total of 57 C57BL/6 wild-type male and female mice were bred in the animal facility at the *Centro de Biología Molecular Severo Ochoa*. They were housed in a specific pathogen-free facility under standard laboratory conditions following European Community Guidelines (directive 86/609/EEC) and handled in accordance with European and local animal care protocols (PROEX 62/14 and 291/15). They were housed 4–5 per cage with food and water available ad libitum and maintained in a temperature-controlled environment on a 12/12-h light/dark cycle with light onset at 8 a.m.

2. *.Experimental design*

The mice were divided into experimental groups (average of 16 months old for the vitamin B12 experiment and 21 months old for the S-(5′-Adenosyl)-L-methionine chloride (SAM), folate, and peptide experiments).

They were randomly injected in the hilus region of both brain hemispheres (2 µl in each one) with vehicle (PBS or distilled water) or one of four molecules of interest: vitamin B12 (50 mg/ml, diluted in water; Vet one, ref: 510218; molecular weight, m.w., 1355 g/mol), SAM (0.25 mg/ml diluted in water; Sigma, ref: A7007; m.w. 398,5 g/mol), folic acid (0.25 mg/ml diluted in PBS; Sigma, ref: F7876-10G; m.w., 441 g/mol), or a synthetic FRα-binding peptide (5 mg/ml, diluted in PBS; Abyntec; m.w., 1121 g/mol). The pH of vitamin B12, methionine, and folic acid solution was adjusted with NaOH to ~7 to avoid negative effects caused by an overly acidic medium. One week after the intracerebral injections, the mice were assessed using behavioral (open field trial) and memory tests (novel object recognition and Y maze test) to determine the potential functional effects of the metabolites on the central nervous system. Two weeks after surgery, the mice were perfused immediately after completing the Y maze test.

3. Stereotaxic surgery and intrahippocampal microinjection

After anesthesia with isoflurane, the mice were secured in a stereotaxic frame (Kopf). Holes were drilled bilaterally in the skull at the injection sites (one per hemisphere) using a microdrill with a 0.5 mm bit. The following stereotaxic coordinates were used for intrahippocampal injections (from bregma): anterior–posterior 2.2; lateral 1.4; and dorsoventral 2.0. A 33-gauge needle Hamilton syringe coupled to a syringe pump controller mounted on the stereotaxic frame was used to inject 2 µl of vehicle or metabolites at each site. Injections were given at 0.25 µl/min, after which the needle was left in place for an additional 3 min, stopping another 3 minutes in the halfway. After the injections, the skin was sutured and buprenorphine (Sigma, USA) was given subcutaneously, and the animals were allowed to recover for 1 h on a heating pad before returning to the cage. Animals were treated with ibuprofen (Dalsy in drinking water) for the following 5 days. The mice remained in the cage for an additional week before the start of behavior tests and were sacrificed 2 weeks after surgery (**SI 1**).

4. CldU injection protocol

The mice received three injections every 2 h (200 ul/injection, intraperitoneally in alternative sites of the body) of 5-Chloro-2'-deoxy-Uridine (CldU, Sigma reference C6891; i.p. 42.75 mg/Kg bodyweight) one week after cranial surgery and microinjections of the solutions and just one week before the sacrifice. This approach allowed us to monitor the effects of the treatments on the proliferation of new cells in the subgranular zone (SGZ), a key region of the brain for neurogenesis, labelling one week-old new generated cells.

5. Animal sacrifice and tissue processing

The mice were anesthetized with an intraperitoneal pentobarbital injection (Dolethal, 60 mg/kg body weight) and transcardially perfused with saline. Brains were separated into two hemispheres. One hemisphere was removed and fixed in 4% paraformaldehyde
in 0.1 M phosphate buffer (PB; pH 7.4) overnight at 4°C. The next day, it was washed three times with 0.1 M PB and cut along the sagittal plane using a vibratome (Leica VT2100S). Serial parasagittal sections (50 mm thick) were cryoprotected in a 30% sucrose solution in PB and stored in ethylene glycol/glycerol at 20°C until they were analyzed. Regarding the other hemisphere, the hippocampus was rapidly dissected on ice and frozen in liquid nitrogen for other studies.

6. Immunofluorescence techniques

For immunofluorescence experiments, free-floating serial sections (50-µm thick) were first rinsed in PB and then pre-incubated for 2 h in PB with 0.25% Triton-X100 and 3% normal serum of the species in which the secondary antibodies were raised (Normal Goat Serum / Normal Donkey Serum, Invitrogen, Thermo Scientific). To study proliferation and neurogenesis, serial sections were previously pre-treated in 2M HCl for 15 min at 30°C. Subsequently, brain sections were incubated for 24 h at 4°C in the same pre-incubation

stock solution (PB+Triton+Serum) containing different combinations of the following primary antibodies: ab6326 (Abcam) for CldU; AB2253 (Sigma Aldrich) for Doublecortin; ab8898 (Abcam) for Histone H3 (tri methyl K9); ab78517 (Abcam) for Histone H4 (di methyl K20, tri methyl K20); TYR1336 Antibody (PhosphoSolution) for NMDA GluN2B Subunit (p1516-1336); ab32423 (Abcam) for brain lipid-binding protein (Blbp); 33D3 (Epigentek) for 5-methylcytosine (5mC); 39791(Active-Motif) for 5-Hydromethylcytosine (5hmC) antibody and L1516 (Merck) for Lectin from *Wisteria floribunda* (WFA).
After rinsing in PB, the sections were incubated for 2 h at room temperature in the appropriate combinations of Alexa 488-594-647-conjugated anti-mouse/rabbit/guinea pig or rat IgG secondary antibodies (1:500; Molecular Probes, Eugene, OR, USA). Sections were also stained with a nuclear stain DAPI (4,6-diamidino-2-phenylindole; Sigma, St. Louis, MO, USA). . In all cases, the sections used were those closest to the injection area and thus in the same positions.
We obtained stitched image stacks from the whole DG at the hippocampus area. These were recorded at 1-µm intervals through separate channels with a 20x lens for the analysis of neurogenesis and the extracellular matrix (ECM) and at 0.45/0.6-µm intervals through separate channels with a 40x lens for the analysis of the NMDA GluN2B subunit, and DNA and histone methylation, respectively (Nikon A1R confocal microscope, NA 0.75, refraction index 1, image resolution: 1024 × 1024 pixels). The same range of z-slices was obtained from each slide in each experiment. Adobe Photoshop (CS4) software was used to build the figures.

7. *Immunohistochemical quantifications*

Dcx/Blbp/CldU-immunoreactive positive cells were quantified by counting the number of cells localized in each DG, distinguishing between the subgranular zone (SGZ), granular cell layer (GCL), and the adjacent hilus region, in four consecutive medial brain sections. For perineuronal nets (PNN) of the ECM, positive units labeled with WFA were counted in the DG (including the GCL and hilus) from three consecutive medial brain sections. To determine the density of different cells, the DG was traced on the DAPI channel of the z projection of each confocal stack of images, and the area of this structure was measured using the freehand drawing tool in Fiji. This area was multiplied by the stack thickness to calculate the reference volume. The number of positive cells was divided by the reference volume, and the density (number of cells/mm^3) of cells was calculated.
For the 5mC, 5hmC, H3K9me3, and H4K20me3 antibodies, confocal settings (laser intensity, gain, pinhole) were kept constant for all images, which were captured in the same confocal session. Using the DAPI channel, the whole GCL area was previously selected as a ROI. An invariant subtract background and threshold was then set in Fiji for each stack projection. The area above the threshold was measured in Fiji and the mean fluorescence in the ROI was calculated and compared between vehicle and folate experimental groups.
For the GluN2B and Sox2 antibodies, the quantification was carried out with the ImageJ program by measuring the percentage of area occupied by the receptor immunoreactivity in the molecular layer of the DG and by YF Sox2 immunoreactivity in the hilus region, SGZ, and GCL. An invariant subtract background and threshold were also set in Fiji for each stack projection.

8. *Nuclear fractionation of cultured human cells*

The method to fractionate the cell nucleus has been previously reported [35], and the presence of FRα-binding peptide in the nuclear fraction was shown by western blot analysis using the antibody against FRα1-binding peptide (Thermo Fisher, ref: PA5-101588).

9. *Nuclear fractionation of cultured human cells and western blotting*

SK-n-sh cells were treated with folate (0.5 or 1mM), FRα-binding peptide (0.5 or 1mM) or DMEM for 30 minutes at 37ºC. Nuclear fractionation was then performed as previously reported [20]. Cell nuclear pellets of each experiment separately was then quantified by the BCA protein assay. Samples were separated on

10% SDS-PAGE and electrophoretically transferred to a nitrocellulose membrane (Schleicher & Schuell GmbH). The membrane was blocked by incubation with 5% semi-fat dried milk in PBS and 0.1% Tween 20 (PBSM), followed by 1-h incubation at room temperature with the primary antibody in PBSM. The following primary antibody dilutions were used: folate receptor alpha 1 (1/300; Thermofisher, ref: PA5-101588). After three washes, the membrane was incubated with a horseradish peroxidase-anti-rabbit Ig conjugate (DAKO), followed by several washes in PBS-Tween 20. The membrane was then incubated for 1 min in Western Lightning reagents (PerkinElmer Life Sciences). Blots were quantified using the EPSON Perfection 1660 scanner and the ImageJ1.46r image analysis system.

10. Behavioral tests

Open field (OF) and novel object recognition (NOR) tests were performed as described previously [36]. Locomotor activity, as well as anxiety and depression-like behavior, was evaluated in old mice using the OF test, which was used as habituation for the NOR test. In brief, on the first day, the mice were placed individually in a 45x45 cm plastic box with vertical opaque walls for 10 min. Each session was recorded, and data like distance, average speed, time immobile, and time on the center square of the box were analyzed with ANY-maze software. On the second day, the mice were placed in the same box for 5 min and allowed to explore two identical objects: A and B (two black rooks, chess piece). The two objects were placed on the long axis of the box each 13 cm from the end of the box. After each exposure, the objects and the box were wiped with 70% ethanol to eliminate odors that could potentially condition the behavior of successive mice. Two hours after the familiarization trial, each mouse was released into the box with the same object previously used (object A) and a new one (object C, a tower of colored plastic pieces), instead of object B (short-term memory test). The position of object C was the same as that of object B in the familiarization trial. The mice were given 5 min to explore the box. Five days later, the mice were released into the box again, with object A in the same position and another new object (object D, a falcon tube filled with wood chips) in the same position as object C in the previous test. Again, the animals were allowed 5 min to explore the box (long-term memory test). They were considered to show recognition when their head was <2 cm from the object, and activity where exploration was less than 1 sec was ruled out.
The memory index (MI) was used to measure recognition memory performance. It was defined as the ratio of time spent exploring or the number of entries in the new object (tC or tD) to the time spent exploring both objects (tA+tC or tA+tD) (MI = [tC/(tA + tC)] X100 and [tD/(tA + tD)] X 100). ANY-maze software was used to calculate the time mice spent exploring the different objects.
To assess spatial memory, a Y maze test based on published protocols with modifications [23] was performed. This test is based on the innate curiosity of rodents to explore novel areas. First, the mice were placed into one of the arms of a black Y-maze apparatus, comprising three plastic arms forming a "Y" shape. They were then allowed to explore the maze for 10 min, with one of the arms closed (training trial). After 1 h, the mice were returned to the same arm of the Y maze (start arm) and were allowed to explore all three arms of the maze for 5 min. The number of entries into and the time spent in each arm were registered on video recordings and analyzed by ANY-maze software. We compared the percentage of time spent in the "novel" arm during the whole trial as a measure of spatial memory performance.

11. Synthetic synthesis of the FRα-binding peptide

To mimic the cognitive results produced by intrahippocampal injection of folate but activating only FRα-binding peptide, we used a synthetic FRα-binding peptide (purity of 90%) with the following sequence: CTVRTSAEC [20]. This peptide was prepared by the company Abyntek (Vizcaya, Spain).

12. Statistical analysis for immunohistochemical and behavior assessments

The data are presented as mean values ± SD. Statistical analyses were performed using GraphPad Prism 8. To compare the two experimental groups (injected with vehicle and with folate or FRα-binding peptide),

an unpaired Student's t test was carried out. A 95% confidence interval was applied for statistical comparisons.

Results

Partial improvement in the object recognition and Y maze tests of mice treated with folate but not with S-Adenosyl-Methionine (SAM) or vitamin B12

SAM, folate, or vehicle was intracranially injected (single dose) into the dorsal hippocampal hilar region (**SI 1**) of old mice. The effects of these injections on behavioral tests were analyzed one week later (see Methods). In the first round of surgeries, we screened SAM treatment in a group of 14 mice. SAM injection had no effect on behavioral performance in the Open Field (OF) test (**Fig. 1a**) or memory (**Fig. 1c**) tests. However, mice treated with folate (n=15; **Fig. 1b and 1d**) showed differences in performance in both tests. In this regard, they showed an improvement in locomotor activity and anxiety-depression-like behavior compared to vehicle-treated mice. **Figure 1d** shows the differences in long-term memory (5 days) in the two tests.

Later, the performance of 12 mice treated with vitamin B12 or vehicle was assessed (**SI 2**). No alteration in locomotor activity (distance traveled, average speed, or time spent immobile) in the OF test or in anxiety-depression-like behavior (time spent in the central square time) was detected in the former group (**SI 2a**). Memory tests (**SI 2b**), focusing on short-term (2 h after training trial) and long-term (5 days after training trial) recognition memory, and on spatial memory did not reveal significant differences between vehicle- and vitamin B12-treated mice.

The result of a single injection of folate was similar to that reported for old mice expressing YF in a cyclical manner [36]. Folate improved the long-term memory (5 days) post-familiarization with the novel object, but no significant differences were found for short-time (2 h) memory (**Fig. 1d**). In addition, folate-treated mice showed improved spatial memory, as reflected by their performance in the Y maze test (**Fig. 1d**). Given our observations that folate injection affected mouse behavior, we examined in greater detail the feasible cellular effects of this compound. To this end, we tested different concentrations of folate. Of note, toxic side effects and even death were observed above 5 mM. We then tested the effect of 2 µl per hemisphere of folate at a concentration of 0.5 mM. This concentration was also used in a previous study [5].

Effect of folate on adult neurogenesis in the dentate gyrus

As in our previous work [36], we tested the effect of folate on neuronal precursor cells, studying changes on brain lipid-binding protein (blbp) (**SI 3a**) and doublecortin-immunoreactive (ir) cell densities. Also, to label dividing cells, mice were injected intraperitoneally with CldU a week before perfusion, thus allowing the study of new-born 1-week-old cells in the SGZ. A single injection of folate into the hippocampus led to only a subtle increase in new-born CldU-ir cells (**SI 3b**) and in 1-week-old neurons (Dcx and CldU double-positive cells) (**SI 3c**) in the SGZ. Although the increase was not statistically significant, the tendency was similar to that found for YF [36]. Furthermore, we found no differences in Blbp-ir (**SI 3a**) or doublecortin-ir cell densities (**SI 3d**) upon folate injection. Therefore, folate had no significant effect on adult hippocampal neurogenesis (AHN).

Indeed, in our previous work [36], a major YF-dependent change was found only in developmentally generated neurons compared to neurons raised in adult neurogenesis in the hippocampal region. Thus, we subsequently tested the effect of folate on developmentally generated cells in the DG, looking at specific markers like changes in histone or DNA methylation.

Impact of folate on the methylation of histone and DNA in hippocampal neurons

The expression of aging-related genes correlates, as suggested by the heterochromatin loss aging model [52], with increasing alterations of chromatin located in heterochromatin regions. In this regard, we examined whether folate injection modifies the degree of histone methylation, namely at positions

H3K9me3 and H4K20me3, which are present mainly in heterochromatin regions. The presence of folate 14 days post-injection did not modify the level of methylation at H3K9me3 (**SI 4a and 4b**) or H4K20me3 (**SI 4c and 4d**).

Our findings suggest that a single injection of folate might not be enough to promote reliable changes in histone methylation levels. Therefore, we tested whether folate affects DNA methylation. Significant increases in 5mC were observed in the granular neuronal layer (P=0.0132) of the DG where the injection was performed (**Fig. 2a, 2a', 2b and 2b'**), and it also tended to increase in the pyramidal layer of CA3 (P-value=0.05) and CA1 (P-value=0.06) (**Fig. 2c, 2d and 2e**)

Regarding 5hmC, we have also tested its levels, since the accumulation of 5hmc in postmitotic neurons is related to "demethylation" (5mc -> 5hmc) facilitating gene expression. No significant changes were found in hippocampal neuronal layers (**SI 5**).

FRα in the cell nucleus could act as a transcription factor

In addition to acting as a methyl donor, folate may exert additional actions on DNA. Upon binding to folate, the folate cell receptor (FRα) [1] can be internalized into the cell nucleus. Nuclear FRα-binding peptide may act as a transcription factor [5]. Using a neuronal human cell line (SK-N-SH) as a model, we confirmed the results reported by Boshnjaku et al. [5], showing that the presence of folate results in the internalization of FRα-binding peptide into the cell nucleus (**SI 6**).

Effect of folate on transcriptional changes

Our objective was to identify a simple compound with the same capacity as YF to improve cognition. In this context, YF are transcriptional factors and nuclear FRα-binding peptide upregulates the expression of YF like Sox2 [26]. In addition, the presence of YF, including Sox2, increases the expression of GluN2B [36].

Furthermore, changes in gene expression occur during aging. Some genes expressed in young cells are no longer expressed, whereas, in old cells, genes that were not previously expressed in young cells could appear. For example, the gene codifying for GluN2B protein is expressed mainly in young neurons [29], whereas genes involved in the formation of PNN are found mostly in aged tissue [45]. Both of them are structures involved in hippocampal neuroplasticity mechanisms.

Changes in GluN2B expression

We previously reported [36] that the presence of YF induces an increase in the expression of GluN2B in the molecular layer of the DG. GluN2B is one of the subunits of the N-methyl-D aspartic acid (NMDA) receptor, which is present mainly in young animals and may be related to greater cognitive capacity [29]. **Figure 3** shows the immunoreactivity of GluN2B in the DG (**Fig. 3a and 3b**) of mice treated or not with folate. GluN2B immunoreactivity in the molecular layer increased in treated animals (**Fig. 3c**)

Changes in extracellular matrix organization

The ECM is organized into perineuronal nets (PNN). These PNN are involved in synaptic stabilization in the mature brain [15]. They comprise proteoglycans like neurocan, brevican, aggrecan, phosphacan, and versican, which can be linked to PNN through their binding to hyaluronan [11, 38]. These PNN can ensheath interneurons, thereby affecting their function [55]. Aging is associated with an increase in PNN in some regions of the brain, including the hippocampus [50, 51]. Thus, we checked the possible reorganization of these structures in response to folate injection. Folate treatment induced a significant reduction in PNN unit density labeled with Wisteria floribunda agglutinin (WFA) lectin in comparison with vehicle-injected counterparts (**Fig. 3d and 3e**).

What is the main effect of folate on cognitive improvement?

To test whether the effect of folate on cognition is due mainly to changes in DNA methylation or to alterations of transcription modulated by factors like nuclear FRα, we tested the effect of an FRα-binding peptide [20] to determine whether it can mimic the effect of folate. To this end, we synthesized a peptide (CTVRTSAEC) able to bind FRα [20]. Although we took into account that the FRα-binding peptide is not a methyl donor and should only facilitate the action of FRα-binding peptide as a transcriptional factor, we first tested, anyway, whether the peptide contributes to DNA methylation. No significant changes in this process were detected (**SI 7**). Thus, we tested whether the peptide induces changes at the transcriptional level. Then, we addressed whether it could also facilitate the internalization of FRα-binding peptide into the cell nucleus. In this regard, we observed that the peptide facilitated FRα uptake into this cell structure, where it may act as a transcription factor (**SI 6**).

Effect of the FRα-binding peptide on SOX2 expression

As previously indicated, folate facilitates the expression of YF, including Sox2 [26]. Thus, we studied whether the FRα-binding peptide affects Sox2 expression. Treatment of aged mice with this peptide resulted in a significant increase in SOX2 expression in various regions of the DG (**Fig. 4a and 4b**).

Effect of the FRα-binding peptide on GLUN2B expression

Given that the presence of YF, such as Sox2, facilitates the expression of GluN2B [36], we addressed whether the presence of the FRα-binding peptide, which upregulates the expression of Sox2, also increases the expression of GluN2B. Treatment with this peptide led to an increase in GLUN2B expression in the molecular layer of the DG (**Fig. 5a, 5b and 5c**), as occurred with folate treatment.

Effect of the FRα-binding peptide on extracellular matrix organization

Previously, it was shown that folate treatment caused changes in ECM organization. The FRα-binding peptide affected this organization in a similar fashion to folate, thereby reducing the density of PNN in the DG (**Fig. 5d and 5e**).
Taking into account the results shown in Figure 5, we suggest that neuronal signaling is enhanced through changes in excitatory (glutamatergic) [29, 36] but also in inhibitory neurons [55]. In addition, both results could be related between them, since alterations in the expression of PNN components during aging, could be modulated by alterations of NMDA function [58].

Cognitive improvement in the presence of FRα-binding peptide

Therefore, we tested whether the treatment with the FRα-binding peptide has a similar effect to that of folate on cognition. Intrahippocampal injection of this peptide under the same conditions as previous folate experiments did not bring about significant changes in short-term memory performance, either in spatial memory or recognition memory, relative to vehicle-treated mice (**Fig. 6a and 6b**). However, treatment with the FRα-binding peptide led to a significant long-term improvement of recognition memory, thereby reproducing the same results as those achieved with folate injections (**Fig. 6c**).

Discussion

Here we devised and tested a novel strategy, involving a simple compound, to replace the YF function of reprogramming old cells to acquire the traits of younger ones. We found that a single injection of folate was a suitable alternative to cyclic treatment with YF. First, folate treatment resulted in epigenetic changes

related to the rejuvenation of methylation patterns, as achieved with YF. Also, we observed an increase in the expression of subunit GluN2B of the NMDA receptor [36, 61]. This subunit is present mainly in excitatory neurons of young animals [46] and this increase may imply enhanced synaptic plasticity, as previously described for YF expression [36]. The increased plasticity induced by the transient presence of folate could underlie the improvement in recognition and spatial memory observed in these old mice. Interestingly, long-term but not short-term recognition memory was enhanced by folate treatment, as occurred with YF cyclical overexpression [36]. Furthermore, aging and age-associated diseases like Alzheimer disease have been related to an increase in perineuronal nets (PNN) in different regions of the brain, including the hippocampus, [22, 45, 50, 51, 58]. PNN are a specific type of ECM wrapped around some interneurons [55] that restrict the plasticity of these cells. PNN are dynamic structures that undergo changes throughout postnatal development, and their reduction has been associated with the facilitation of neuronal plasticity and memory enhancement [37, 38, 47]. In this regard, our results in aged mice showing the reorganization of the ECM by reducing the density of PNN replicate those reported for the rejuvenating effects of YF on the hippocampus [36].

The mechanism for YF reprogramming could involve transcriptional changes and an increase in DNA methylation [24, 48, 57]. Given that the latter process can also be enhanced by the presence of methyl donors or cofactors, we tested the possible reprogramming effect of folate and SAM as methyl donor and of vitamin B12 as a cofactor. Although methionine is the universal methyl donor, folate may act as a donor through folate-methionine metabolism [13]. However, some differences between the presence of methionine and folate can be found. Toxicity for high levels of methionine but not for folate were found in humans [16]. Methionine toxicity could be due to the fact that methionine is a precursor of the toxic homocysteine [30]. Also, it should be noted that a high-methionine diet induces Alzheimer disease-like symptoms [31]. On the other hand, other side effects can occur; for example, if methionine is converted to SAM, the latter can also remethylate methionine through homocysteine [13, 28]. Also, there is a decrease in the levels of folate and an increase in homocysteine with age [13]. In addition, low levels of folate may correlate with the cognitive decline of elderly patients [2]. In fact, folate supplement has been proposed as a potential treatment for improving memory deficits [10, 14]. On the other hand, the link between vitamin B12, folate, and homocysteine and cognitive performance during aging is well known [34].

Of note, despite the involvement of both folate and SAM as possible methyl donors, only folate was found to have a similar impact on cognition as YF. This difference could be explained by the interaction of this compound with the folate receptors, FRα being the most relevant. FRα is a transcription factor that is involved in the expression of the YF Sox2 [26]. The same long-term recognition memory enhancement induced by treatment with FRα-binding peptide as with folate injections would also support this hypothesis. Folate deficiency related to aging may result in the exposure of hypomethylated DNA present in heterochromatin regions, after despiralization of chromatin [13]. In this way, aging has been related to a loss of DNA methylation [4, 56], particularly at constitutive heterochromatin [49, 52, 53], which may potentially lead to altered chromatin functioning and genomic instability [19]. In this regard, in the model of aging due to the loss of heterochromatin, heterochromatin markers like DNA methylation decrease with age at the time of heterochromatin loss [52].Otherwise, aging could be also related to an increase in DNA methylation, mainly in euchromatin regions [17].

Indeed, loss of heterochromatin has been found in premature aging disorders like Hutchinson-Gilford progeria [40, 42] and Werner syndrome [61]. Heterochromatin markers like DNA cytosine-5 methylation are globally decreased in the hippocampus during aging [6, 43], leading to general DNA hypomethylation [9]. The latter may facilitate the presence of aging signatures [21, 60], but if DNA methylation is promoted, these signatures may be corrected. However, our results suggest that the main effect of folate on cognition is not due mainly to general changes in DNA methylation but to its action on FRα, which can increase the levels of factors like GLUN2B, or produce changes in the organization of the ECM, specifically PNN, which, in addition, will improve cognitive functions such as long-term memory. Thus, our current working hypothesis indicates a possible pathway to explain the role of folate or the FRα-binding peptide in cognitive improvement of old mice, described in the following pathway: <u>folate or peptide</u>, <u>nuclear FRα</u>, <u>Sox2↑</u>, <u>GluN2B ↑</u>, <u>ECM organization ↓</u>, <u>improved cognition</u>.

We observed several similarities and differences between the addition of folate and FR-binding peptide in our working hypothesis (**Fig. 7**). In this context, we propose that folate and/or the indicated FRα-binding

peptide promote cognition, mainly through the action of nuclear FRα. However, for folate, we cannot rule out that changes at the DNA methylation level may help to facilitate this functional improvement. In fact, folate treatment led not only to enhanced recognition memory but also better spatial memory when compared to the results of the mice treated with the FRα-binding peptide. On the other hand, we have not find, up to now, any negative side effects caused by treatment with this peptide.

In summary, of the three possible effects of folate on cognitive improvement tested: a) increasing trend in adult neurogenesis, b) increase in DNA methylation or c) increase in neuroplasticity by reorganizing extracellular matrix structures of rising the expression of juvenile genes like GluN2B, we suggest that effect c) could play the main role in cognitive improvement.

In conclusion, our results indicate that folate or FRα-peptide binding treatment can reprogram aged DG cells and thus enhance cognitive improvement. Thus, Folate or FRα peptide emerge as an alternative strategy to treatment with YF.

Ethic declarations

1. Competing interest

The authors declare that they have no competing interests to disclose.

2. Ethical approval

All applicable international, national, and institutional animal welfare guidelines were followed for the experiments involving experimentation animals. All procedures were in accordance with ethical standards and were approved by the pertinent Ethics Committee. Mice were bred in the animal facility of Centro de Biología Molecular Severo Ochoa. They were housed in a specific pathogen-free colony facility under standard laboratory conditions, following European Community Guidelines (directive 86/609/EEC), and handled in accordance with European and local animal care protocols (PROEX 102.0/21). 4–5 mice were housed per cage with food and water available ad libitum, and maintained in a temperature-controlled environment on a 12h/12h light/dark cycle with light onset at 8 a.m.

506 **Reference list**
507

508 1 Alam C, Aufreiter S, Georgiou CJ, Hoque MT, Finnell RH, O'Connor DL, Goldman ID, Bendayan
509 R (2019) Upregulation of reduced folate carrier by vitamin D enhances brain folate uptake in mice
510 lacking folate receptor alpha. Proc Natl Acad Sci U S A 116: 17531-17540 Doi
511 10.1073/pnas.1907077116
512 2 Araujo JR, Martel F, Borges N, Araujo JM, Keating E (2015) Folates and aging: Role in mild
513 cognitive impairment, dementia and depression. Ageing Res Rev 22: 9-19 Doi
514 10.1016/j.arr.2015.04.005
515 3 Benayoun BA, Pollina EA, Brunet A (2015) Epigenetic regulation of ageing: linking
516 environmental inputs to genomic stability. Nat Rev Mol Cell Biol 16: 593-610 Doi
517 10.1038/nrm4048
518 4 Bollati V, Schwartz J, Wright R, Litonjua A, Tarantini L, Suh H, Sparrow D, Vokonas P,
519 Baccarelli A (2009) Decline in genomic DNA methylation through aging in a cohort of elderly
520 subjects. Mech Ageing Dev 130: 234-239 Doi 10.1016/j.mad.2008.12.003
521 5 Boshnjaku V, Shim KW, Tsurubuchi T, Ichi S, Szany EV, Xi G, Mania-Farnell B, McLone DG,
522 Tomita T, Mayanil CS (2012) Nuclear localization of folate receptor alpha: a new role as a
523 transcription factor. Sci Rep 2: 980 Doi 10.1038/srep00980
524 6 Chen H, Dzitoyeva S, Manev H (2012) Effect of aging on 5-hydroxymethylcytosine in the mouse
525 hippocampus. Restor Neurol Neurosci 30: 237-245 Doi 10.3233/RNN-2012-110223
526 7 Chen R, Skutella T (2022) Synergistic Anti-Ageing through Senescent Cells Specific
527 Reprogramming. Cells 11: 830 Doi 10.3390/cells11050830
528 8 Chondronasiou D, Gill D, Mosteiro L, Urdinguio RG, Berenguer-Llergo A, Aguilera M, Durand
529 S, Aprahamian F, Nirmalathasan N, Abad Met al (2022) Multi-omic rejuvenation of naturally aged
530 tissues by a single cycle of transient reprogramming. Aging Cell 21: e13578 Doi
531 10.1111/acel.13578
532 9 Ciccarone F, Tagliatesta S, Caiafa P, Zampieri M (2018) DNA methylation dynamics in aging:
533 how far are we from understanding the mechanisms? Mech Ageing Dev 174: 3-17 Doi
534 10.1016/j.mad.2017.12.002
535 10 Cummings J, Scheltens P, McKeith I, Blesa R, Harrison JE, Bertolucci PH, Rockwood K,
536 Wilkinson D, Wijker W, Bennett DAet al (2017) Effect Size Analyses of Souvenaid in Patients
537 with Alzheimer's Disease. J Alzheimers Dis 55: 1131-1139 Doi 10.3233/JAD-160745
538 11 Deepa SS, Carulli D, Galtrey C, Rhodes K, Fukuda J, Mikami T, Sugahara K, Fawcett JW (2006)
539 Composition of perineuronal net extracellular matrix in rat brain: a different disaccharide
540 composition for the net-associated proteoglycans. J Biol Chem 281: 17789-17800 Doi
541 10.1074/jbc.M600544200
542 12 Ducker GS, Rabinowitz JD (2017) One-Carbon Metabolism in Health and Disease. Cell Metab
543 25: 27-42 Doi 10.1016/j.cmet.2016.08.009
544 13 Fenech M (2010) Folate, DNA damage and the aging brain. Mech Ageing Dev 131: 236-241 Doi
545 10.1016/j.mad.2010.02.004
546 14 Fioravanti M, Ferrario E, Massaia M, Cappa G, Rivolta G, Grossi E, Buckley AE (1998) Low
547 folate levels in the cognitive decline of elderly patients and the efficacy of folate as a treatment
548 for improving memory deficits. Arch Gerontol Geriatr 26: 1-13 Doi 10.1016/s0167-
549 4943(97)00028-9
550 15 Flores CE, Mendez P (2014) Shaping inhibition: activity dependent structural plasticity of
551 GABAergic synapses. Front Cell Neurosci 8: 327 Doi 10.3389/fncel.2014.00327
552 16 Garlick PJ (2006) Toxicity of methionine in humans. J Nutr 136: 1722S-1725S Doi
553 10.1093/jn/136.6.1722S
554 17 Horvath S, Raj K (2018) DNA methylation-based biomarkers and the epigenetic clock theory of
555 ageing. Nat Rev Genet 19: 371-384 Doi 10.1038/s41576-018-0004-3
556 18 Hou P, Li Y, Zhang X, Liu C, Guan J, Li H, Zhao T, Ye J, Yang W, Liu Ket al (2013) Pluripotent
557 stem cells induced from mouse somatic cells by small-molecule compounds. Science 341: 651-
558 654 Doi 10.1126/science.1239278
559 19 Hu Z, Chen K, Xia Z, Chavez M, Pal S, Seol JH, Chen CC, Li W, Tyler JK (2014) Nucleosome
560 loss leads to global transcriptional up-regulation and genomic instability during yeast aging. Genes
561 Dev 28: 396-408 Doi 10.1101/gad.233221.113
562 20 Hulin-Curtis SL, Davies JA, Nestic D, Bates EA, Baker AT, Cunliffe TG, Majhen D, Chester JD,
563 Parker AL (2020) Identification of folate receptor alpha (FRalpha) binding oligopeptides and their
564 evaluation for targeted virotherapy applications. Cancer Gene Ther 27: 785-798 Doi
565 10.1038/s41417-019-0156-0

21 Johansson A, Enroth S, Gyllensten U (2013) Continuous Aging of the Human DNA Methylome Throughout the Human Lifespan. PLoS One 8: e67378 Doi 10.1371/journal.pone.0067378

22 Karetko-Sysa M, Skangiel-Kramska J, Nowicka D (2014) Aging somatosensory cortex displays increased density of WFA-binding perineuronal nets associated with GAD-negative neurons. Neuroscience 277: 734-746 Doi 10.1016/j.neuroscience.2014.07.049

23 Kraeuter AK, Guest PC, Sarnyai Z (2019) The Y-Maze for Assessment of Spatial Working and Reference Memory in Mice. Methods Mol Biol 1916: 105-111 Doi 10.1007/978-1-4939-8994-2_10

24 Lopez-Bertoni H, Lal B, Li A, Caplan M, Guerrero-Cazares H, Eberhart CG, Quinones-Hinojosa A, Glas M, Scheffler B, Laterra Jet al (2015) DNMT-dependent suppression of microRNA regulates the induction of GBM tumor-propagating phenotype by Oct4 and Sox2. Oncogene 34: 3994-4004 Doi 10.1038/onc.2014.334

25 Lopez-Otin C, Blasco MA, Partridge L, Serrano M, Kroemer G (2013) The hallmarks of aging. Cell 153: 1194-1217 Doi 10.1016/j.cell.2013.05.039

26 Mohanty V, Shah A, Allender E, Siddiqui MR, Monick S, Ichi S, Mania-Farnell B, D GM, Tomita T, Mayanil CS (2016) Folate Receptor Alpha Upregulates Oct4, Sox2 and Klf4 and Downregulates miR-138 and miR-let-7 in Cranial Neural Crest Cells. Stem Cells 34: 2721-2732 Doi 10.1002/stem.2421

27 Ocampo A, Reddy P, Martinez-Redondo P, Platero-Luengo A, Hatanaka F, Hishida T, Li M, Lam D, Kurita M, Beyret Eet al (2016) In Vivo Amelioration of Age-Associated Hallmarks by Partial Reprogramming. Cell 167: 1719-1733 e1712 Doi 10.1016/j.cell.2016.11.052

28 Ostrakhovitch EA, Tabibzadeh S (2019) Homocysteine and age-associated disorders. Ageing Res Rev 49: 144-164 Doi 10.1016/j.arr.2018.10.010

29 Paoletti X, Oba K, Bang YJ, Bleiberg H, Boku N, Bouche O, Catalano P, Fuse N, Michiels S, Moehler Met al (2013) Progression-free survival as a surrogate for overall survival in advanced/recurrent gastric cancer trials: a meta-analysis. J Natl Cancer Inst 105: 1667-1670 Doi 10.1093/jnci/djt269

30 Perna AF, Ingrosso D, Lombardi C, Acanfora F, Satta E, Cesare CM, Violetti E, Romano MM, De Santo NG (2003) Possible mechanisms of homocysteine toxicity. Kidney Int Suppl: S137-140 Doi 10.1046/j.1523-1755.63.s84.33.x

31 Pi T, Wei S, Jiang Y, Shi JS (2021) High Methionine Diet-Induced Alzheimer's Disease like Symptoms Are Accompanied by 5-Methylcytosine Elevated Levels in the Brain. Behav Neurol 2021: 6683318 Doi 10.1155/2021/6683318

32 Planello AC, Ji J, Sharma V, Singhania R, Mbabaali F, Muller F, Alfaro JA, Bock C, De Carvalho DD, Batada NN (2014) Aberrant DNA methylation reprogramming during induced pluripotent stem cell generation is dependent on the choice of reprogramming factors. Cell Regen 3: 4 Doi 10.1186/2045-9769-3-4

33 Pollina EA, Brunet A (2011) Epigenetic regulation of aging stem cells. Oncogene 30: 3105-3126 Doi 10.1038/onc.2011.45

34 Riggs KM, Spiro A, 3rd, Tucker K, Rush D (1996) Relations of vitamin B-12, vitamin B-6, folate, and homocysteine to cognitive performance in the Normative Aging Study. Am J Clin Nutr 63: 306-314 Doi 10.1093/ajcn/63.3.306

35 Ritter ML, Avila J, Garcia-Escudero V, Hernandez F, Perez M (2018) Frontotemporal Dementia-Associated N279K Tau Mutation Localizes at the Nuclear Compartment. Front Cell Neurosci 12: 202 Doi 10.3389/fncel.2018.00202

36 Rodriguez-Matellan A, Alcazar N, Hernandez F, Serrano M, Avila J (2020) In Vivo Reprogramming Ameliorates Aging Features in Dentate Gyrus Cells and Improves Memory in Mice. Stem Cell Reports 15: 1056-1066 Doi 10.1016/j.stemcr.2020.09.010

37 Romberg C, Yang S, Melani R, Andrews MR, Horner AE, Spillantini MG, Bussey TJ, Fawcett JW, Pizzorusso T, Saksida LM (2013) Depletion of perineuronal nets enhances recognition memory and long-term depression in the perirhinal cortex. J Neurosci 33: 7057-7065 Doi 10.1523/JNEUROSCI.6267-11.2013

38 Rowlands D, Lensjo KK, Dinh T, Yang S, Andrews MR, Hafting T, Fyhn M, Fawcett JW, Dick G (2018) Aggrecan Directs Extracellular Matrix-Mediated Neuronal Plasticity. J Neurosci 38: 10102-10113 Doi 10.1523/JNEUROSCI.1122-18.2018

39 Sarkar TJ, Quarta M, Mukherjee S, Colville A, Paine P, Doan L, Tran CM, Chu CR, Horvath S, Qi LSet al (2020) Transient non-integrative expression of nuclear reprogramming factors promotes multifaceted amelioration of aging in human cells. Nat Commun 11: 1545 Doi 10.1038/s41467-020-15174-3

40 Scaffidi P, Misteli T (2005) Reversal of the cellular phenotype in the premature aging disease Hutchinson-Gilford progeria syndrome. Nat Med 11: 440-445 Doi 10.1038/nm1204
41 Sen P, Shah PP, Nativio R, Berger SL (2016) Epigenetic Mechanisms of Longevity and Aging. Cell 166: 822-839 Doi 10.1016/j.cell.2016.07.050
42 Shumaker DK, Dechat T, Kohlmaier A, Adam SA, Bozovsky MR, Erdos MR, Eriksson M, Goldman AE, Khuon S, Collins FSet al (2006) Mutant nuclear lamin A leads to progressive alterations of epigenetic control in premature aging. Proc Natl Acad Sci U S A 103: 8703-8708 Doi 10.1073/pnas.0602569103
43 Szulwach KE, Li X, Li Y, Song CX, Wu H, Dai Q, Irier H, Upadhyay AK, Gearing M, Levey AIet al (2011) 5-hmC-mediated epigenetic dynamics during postnatal neurodevelopment and aging. Nat Neurosci 14: 1607-1616 Doi 10.1038/nn.2959
44 Takahashi K, Yamanaka S (2006) Induction of pluripotent stem cells from mouse embryonic and adult fibroblast cultures by defined factors. Cell 126: 663-676 Doi 10.1016/j.cell.2006.07.024
45 Tanaka Y, Mizoguchi K (2009) Influence of aging on chondroitin sulfate proteoglycan expression and neural stem/progenitor cells in rat brain and improving effects of a herbal medicine, yokukansan. Neuroscience 164: 1224-1234 Doi 10.1016/j.neuroscience.2009.08.060
46 Tang YP, Shimizu E, Dube GR, Rampon C, Kerchner GA, Zhuo M, Liu G, Tsien JZ (1999) Genetic enhancement of learning and memory in mice. Nature 401: 63-69 Doi 10.1038/43432
47 Thompson EH, Lensjo KK, Wigestrand MB, Malthe-Sorenssen A, Hafting T, Fyhn M (2018) Removal of perineuronal nets disrupts recall of a remote fear memory. Proc Natl Acad Sci U S A 115: 607-612 Doi 10.1073/pnas.1713530115
48 Tsai CC, Su PF, Huang YF, Yew TL, Hung SC (2012) Oct4 and Nanog directly regulate Dnmt1 to maintain self-renewal and undifferentiated state in mesenchymal stem cells. Mol Cell 47: 169-182 Doi 10.1016/j.molcel.2012.06.020
49 Tsurumi A, Li WX (2012) Global heterochromatin loss: a unifying theory of aging? Epigenetics 7: 680-688 Doi 10.4161/epi.20540
50 Ueno H, Suemitsu S, Murakami S, Kitamura N, Wani K, Takahashi Y, Matsumoto Y, Okamoto M, Ishihara T (2019) Alteration of Extracellular Matrix Molecules and Perineuronal Nets in the Hippocampus of Pentylenetetrazol-Kindled Mice. Neural Plast 2019: 8924634 Doi 10.1155/2019/8924634
51 Vegh MJ, Rausell A, Loos M, Heldring CM, Jurkowski W, van Nierop P, Paliukhovich I, Li KW, del Sol A, Smit ABet al (2014) Hippocampal extracellular matrix levels and stochasticity in synaptic protein expression increase with age and are associated with age-dependent cognitive decline. Mol Cell Proteomics 13: 2975-2985 Doi 10.1074/mcp.M113.032086
52 Villeponteau B (1997) The heterochromatin loss model of aging. Exp Gerontol 32: 383-394 Doi 10.1016/s0531-5565(96)00155-6
53 Wang J, Jia ST, Jia S (2016) New Insights into the Regulation of Heterochromatin. Trends Genet 32: 284-294 Doi 10.1016/j.tig.2016.02.005
54 Watanabe A, Yamada Y, Yamanaka S (2013) Epigenetic regulation in pluripotent stem cells: a key to breaking the epigenetic barrier. Philos Trans R Soc Lond B Biol Sci 368: 20120292 Doi 10.1098/rstb.2012.0292
55 Wen TH, Binder DK, Ethell IM, Razak KA (2018) The Perineuronal 'Safety' Net? Perineuronal Net Abnormalities in Neurological Disorders. Front Mol Neurosci 11: 270 Doi 10.3389/fnmol.2018.00270
56 Wilson VL, Jones PA (1983) DNA methylation decreases in aging but not in immortal cells. Science 220: 1055-1057 Doi 10.1126/science.6844925
57 Wu F, Wu Q, Li D, Zhang Y, Wang R, Liu Y, Li W (2018) Oct4 regulates DNA methyltransferase 1 transcription by direct binding of the regulatory element. Cell Mol Biol Lett 23: 39 Doi 10.1186/s11658-018-0104-2
58 Yamada J, Ohgomori T, Jinno S (2017) Alterations in expression of Cat-315 epitope of perineuronal nets during normal ageing, and its modulation by an open-channel NMDA receptor blocker, memantine. J Comp Neurol 525: 2035-2049 Doi 10.1002/cne.24198
59 Yamanaka S (2008) Induction of pluripotent stem cells from mouse fibroblasts by four transcription factors. Cell Prolif 41 Suppl 1: 51-56 Doi 10.1111/j.1365-2184.2008.00493.x
60 Zampieri M, Ciccarone F, Calabrese R, Franceschi C, Burkle A, Caiafa P (2015) Reconfiguration of DNA methylation in aging. Mech Ageing Dev 151: 60-70 Doi 10.1016/j.mad.2015.02.002
61 Zhang W, Li J, Suzuki K, Qu J, Wang P, Zhou J, Liu X, Ren R, Xu X, Ocampo Aet al (2015) Aging stem cells. A Werner syndrome stem cell model unveils heterochromatin alterations as a driver of human aging. Science 348: 1160-1163 Doi 10.1126/science.aaa1356

685 **Figure legends**
686
687
688 **Figure 1. Effect of methyl donors SAM and folate on behavior**. Old wild-type mice receiving a single
689 dose of of folate via hippocampal infusion showed behavioral changes when compared with mice treated
690 with vehicle solution. This observation was not made for S-adenosylmethionine metabolite (SAM)
691 infusion. (**a, b**) Histograms show some of the main data from the open field test: time spent by mice in the
692 center square of the box, average speed of movement, and time spent immobile. Folate-treated mice
693 showed an improvement in anxiety-depression-like behavior (indicated by the time spent in the center
694 square), as well as in general motor activity (illustrated by the rest of the histograms).
695 (**c, d**) Histograms show results from two memory tests: namely the novel object recognition test (NOR) for
696 short and long-term recognition memory, and the Y maze test for spatial memory. Significant differences
697 were found in folate-treated mice in comparison with the vehicle-treated group, but none were found
698 between SAM-treated and vehicle-treated mice in any memory test. Black bars represent mean± SD of
699 vehicle-treated group and gray bar the mean± SD of SAM/Folate-treated group. All data were analyzed by
700 Student`s t-tests. *p<0.05, **p<0.01.
701
702 **Figure 2. Effect of folate on DNA methylation of hippocampal neurons.** (**a, b**) Representative stitched
703 confocal images of 5-Methylcytosine (5mC) marker (in green) in the dentate gyrus of vehicle-treated and
704 folate-treated mice. **a'** and **b'** are the corresponding higher magnifications of the granular cell layer of a
705 and b (white squares). Heterochromatin clusters of 5mC immunoreactivity can be observed in a' and b. (**c,**
706 **d, e**) Histogram showing mean intensity of the 5mC signal in the granular cell layer of the DG, and in the
707 pyramidal cell layer of CA3 and CA1 hippocampal regions. The effect of the absence (black) or presence
708 (gray) of folic acid is shown. (Mean±SD; *p<0.05, Student`s t test; ns: no significant differences). Scale
709 bar, 100 µm (A and B) and 10 µm (A' and B').
710
711 **Figure 3. Effects of folate on GluN2B expression and extracellular matrix organization.** Effects on
712 folate on the presence of the NMDA receptor subunit GluN2B in mature hippocampal neurons. (**a, b**)
713 Representative stitched confocal images of GluN2B distribution in the dentate gyrus (DG) of old wild-type
714 mice treated with vehicle or folate. **a'** and **b'** are the corresponding higher magnifications of the molecular
715 cell layer of a and b (white squares). (**c**) Histogram showing the percentage of area occupied by GluN2B
716 signal in the molecular layer of the DG. The effect of the absence (black) or presence (gray) of folic acid is
717 shown. Treatment with folate induced a significant increase in GluN2B expression in the DG (Mean±SD;
718 *p<0.05, Student`s t test). **(d)** Representative stitched confocal images of Wisteria floribunda agglutinin
719 (WFA, in green), as a marker of perineuronal nets (PNN) in the DG of vehicle-treated and folate-treated
720 mice. Nuclear marker DAPI is shown in blue. (**e**) Single-dose treatment with folate resulted in statistically
721 significant changes in PNN density at the DG (Mean±SD; *p<0.05, Student`s t test). Scale bars, 100 µm
722 (a, b, d) and 10 µm (a' and b').
723
724 **Figure 4. Effect of FRα-binding peptide on the expression of Yamanaka factor Sox2.**
725 **(a)** Representative stitched confocal images of Sox2 expression (in red) in the dentate gyrus (DG) of
726 vehicle-treated and FRα-treated mice. Nuclear marker DAPI is shown in blue. (**b**) Single-dose treatment
727 with FRα-binding peptide resulted in statistically significant changes in Sox2 immunoreactivity expression
728 in the hilus region, granular cell layer (GCL), and subgranular zone (SGZ) of the DG. (Mean±SD; *p<0.05,
729 **p<0.01; Student`s t test). Scale bar, 100 µm.
730
731 **Figure 5. Effects of folate receptor α (FRα)-binding peptide on GluN2B expression and extracellular**
732 **matrix organization.** Effects of the FRα-binding peptide on the presence of the NMDA receptor subunit
733 GluN2B in mature hippocampal neurons. (**a, b**) Representative stitched confocal images of GluN2B
734 distribution in the dentate gyrus (DG) of old wild-type mice treated with vehicle or FRα-binding peptide.
735 **a'** and **b'** are the corresponding higher magnifications of the molecular cell layer of A and B (white
736 squares). (**c**) Histogram showing the percentage of area occupied by the GluN2B signal in the molecular
737 layer of the DG. The effect of the absence (black) or presence (gray) of FRα is shown. Treatment with FRα-

738 binding peptide induced a significant increase in GluN2B expression in the DG (Mean±SD; *p<0.05,
739 Student`s t test). **(d)** Representative stitched confocal images of Wisteria floribunda agglutinin (WFA, in
740 green), as a marker of perineuronal nets (PNN) in the DG of mice injected with vehicle or FRα-binding
741 peptide. Nuclear marker DAPI is shown in blue. (**e**) Single-dose treatment with FRα-binding peptide
742 resulted in statistically significant changes in PNN density at the DG. (Mean±SD; *p<0.05, **p<0.01;
743 Student`s t test). Scale bar, 100 µm (A, B and D) and 10 µm (A' and B').
744
745 **Figure 6. Effect of FRα-binding peptide on cognition.**
746 Histograms show results from two memory tests: the Y-maze test for spatial memory (**a**) and the novel
747 object recognition (NOR) for short- (**b**) and long-term recognition memory (**c**). Mice treated with the
748 peptide showed a significant improvement in memory retention after 5 days since first training, as shown
749 by memory index of novel object recognition test. Treatment with FRα-binding peptide did not have a
750 significant effect on short-term recognition memory or spatial memory. Black bars represent mean± SD of
751 vehicle-treated group and gray bars represent mean± SD of the peptide-treated group. All data were
752 analyzed by Student`s t-tests. *p<0.05
753
754 **Figure 7. Scheme of main results**. Left- According to the heterochromatin loss aging model [52],
755 heterochromatin biomarkers like DNA methylation (in heterochromatin regions) are lost with age. Right-
756 At the same time, during aging, the brain undergoes changes in DNA expression, leading to decreased
757 levels of certain genes, like GluN2B, related with more juvenile states or with increased levels of other
758 structures like perineuronal nets (PNN).
759 Center- In this work, we report that folate and the FRα-binding peptide may facilitate the transport of FRα-
760 binding peptide to the cell nucleus, where the receptor acts like a transcription factor [5]. Consequently,
761 treatment with either of these two compounds reverted the age-associated loss of neuroplasticity by
762 changing expression in GluN2B and in PNN units, thereby leading to cognitive improvement. Furthermore,
763 treatment with folate but not with the FRα-binding peptide led to a significant increase in DNA methylation,
764 thereby recovering the heterochromatin loss associated with aging.
765
766
767 **Supplementary Figure 1. Experimental timeline and intracerebral injections. (a)** Schematic
768 illustration of the experimental timeline of experiments performed in the present work. **(b)** IIllustration
769 (modified from Paxinos, George, and Keith B.J. Franklin). The mouse brain in stereotaxic coordinates: hard
770 cover edition. (Access Online via Elsevier, 2001) of anatomical localization of the bilateral monodose
771 injections (red plot) performed in the Dentate Gyrus (Anteroposterior -2 mm; Mediolateral ±1.4 mm;
772 Dorsoventral -2.2 mm) of different metabolites (vitamin B12, SAM, and folate) and of FRα-binding peptide
773 or vehicle solution, in wild-type mice (male and female were randomized into experimental groups). On
774 the bottom it is shown representative examples of trial hippocampal injections with dextran tracer (in red)
775 performed before the start of the treatments. Note the trajectory of the 5ul Hamilton syringe, which only
776 reaches the hilus of the DG.
777
778 **Supplementary Figure 2. Effect of vitamin B12 on behavior.** Single dose of hippocampal infusions of
779 vitamin B12 did not alter the behavior of old wild-type mice compared with mice receiving vehicle
780 solution. (**a**) Histograms show some of the main data from the open field test: time spent by mice in the
781 center square of the box during the test, average speed of movement, and time spent immobile. (**b**)
782 Histograms show results from two memory performance tests: the novel object recognition test (NOR) for
783 short- and long-term recognition memory, and the Y maze test for spatial memory. Black bars represent
784 mean± SD of vehicle-treated group and gray bars represent mean± SD of the vitamin B12-treated group.
785 All data were analyzed by Student`s t-tests.
786
787 **Supplementary Figure 3. Effect of folate on the expression of adult neurogenesis markers**. (**a**)
788 Histogram showing density of Blbp-ir cells per mm^3 obtained in the subgranular zone (SGZ) of the dentate
789 gyrus. Single-dose treatment with folate did not cause statistically significant changes in early neural
790 precursors in the SGZ. (**b**) Histogram showing density of CldU-ir cells per mm^3 in the SGZ. Single-dose

treatment with folate did not cause statistically significant changes in the generation of new cells in the SGZ. (**c**) Histogram showing percentage of doublecortin-ir cells that were also CldU-immunoreactive in the SGZ. Single-dose treatment with folate did not cause statistically significant changes in the density of new 2-week-old neurons in the SGZ. (**d**) Histogram showing density of doublecortin-ir cells per mm^3 in the SGZ. Single-dose treatment with folate did not cause statistically significant changes in the density of young neurons in the SGZ. (Mean±SD; ns: not significant differences; Student`s t test).

Supplementary Figure 4. Levels of H3K9me3 and H4K20me3. Effect of folate. (**a**) Representative stitched confocal images of H3K9me3 marker (in red) in the dentate gyrus (DG). Inset also shows DAPI signal (in blue) to identify the DG structure. (**b**) Histogram showing mean intensity of histone methylation signal. The effect of the absence (black) or presence (gray) of folic acid is shown. (**c**) Representative stitched confocal images of the H4K20me3 marker (in green) in the DG. Inset also shows the DAPI signal (in blue) to identify the DG structure. (**d**) Histogram showing mean intensity of histone methylation signal. The effect of the absence (black) or presence (gray) of folic acid is shown. (Mean±SD; ns: not significant differences; Student`s t test). Scale bar, 100 µm.

Supplementary Figure 5. Levels of 5hmC. Effect of folate. (**a**) Representative stitched confocal images of 5-hydroxymethylcytosine (5hmC) marker (in red) in the dentate gyrus (DG) of vehicle-treated and folate-treated mice. (**b**) Histogram showing mean intensity from 5mC signal of the granular cell layer of the DG. The effect of the absence (black) or presence (gray) of folic acid is shown. (Mean±SD; *$p<0.05$, Student`s t test; ns: not significant differences). Scale bar, 100 µm.

Supplementary Figure 6. Expression of the FRα-binding peptide on nuclear fraction by addition of folate or the FRα-binding peptide. Boshnjaku et al.[5] described that, that upon folate addition, FRα-binding peptide (which appears as two bands around 42kd and 38Kd) can be internalized to the cytoplasm (~42 Kd band) or the nucleus (~38Kd band). We therefore studied the localization of FRα-binding peptide upon addition to SK-N-SH human neuroblastoma cells of two concentrations of folate and FRα-binding peptide (0.5 (+) and 1 (++) mM). Our results show the presence of ~38Kd band in the nuclear fraction (**a**) in the presence or absence of folate or FRα-binding peptide at different concentrations. (**b**) Quantification of the results of A. Results of densitometry were normalized against the control value.

Supplementary Figure 7. Levels of 5mC and 5hmC. Effect of the FRα-binding peptide. Histograms showing mean intensity from 5mC (**a**) and 5hmC (**b**) signal of the granular cell layer of the dentate gyrus (DG) region. The effect of the absence (black) or presence (gray) of the FRα-binding peptide (2,5mg/ml) is shown. No significant effect on DNA methylation status of the DG was found. (Mean±SD; *$p<0.05$, Student`s t test; ns: no significant differences).

Fig.1

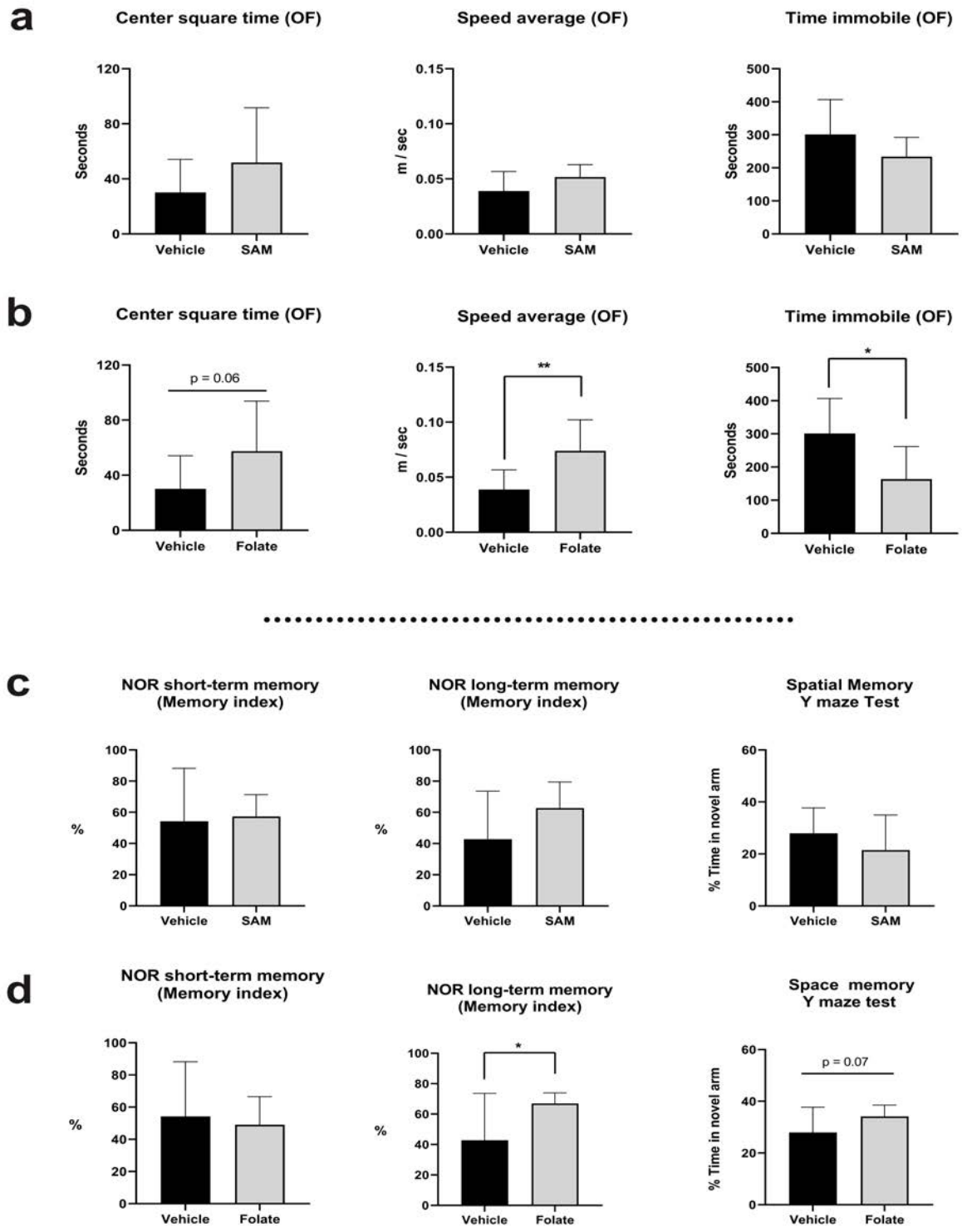
a
Center square time (OF)
Seconds
120
80
40
0
Vehicle
SAM
Speed average (OF)
m / sec
0.15
0.10
0.05
0.00
Vehicle
SAM
Time immobile (OF)
Seconds
500
400
300
200
100
0
Vehicle
SAM
b
Center square time (OF)
p = 0.06
Seconds
120
80
40
0
Vehicle
Folate
Speed average (OF)
**
m / sec
0.15
0.10
0.05
0.00
Vehicle
Folate
Time immobile (OF)
*
Seconds
500
400
300
200
100
0
Vehicle
Folate
c
NOR short-term memory
(Memory index)
%
100
80
60
40
20
0
Vehicle
SAM
NOR long-term memory
(Memory index)
%
100
80
60
40
20
0
Vehicle
SAM
Spatial Memory
Y maze Test
% Time in novel arm
60
40
20
0
Vehicle
SAM
d
NOR short-term memory
(Memory index)
%
100
80
60
40
20
0
Vehicle
Folate
NOR long-term memory
(Memory index)
*
%
100
80
60
40
20
0
Vehicle
Folate
Space memory
Y maze test
p = 0.07
% Time in novel arm
60
40
20
0
Vehicle
Folate

Fig.2

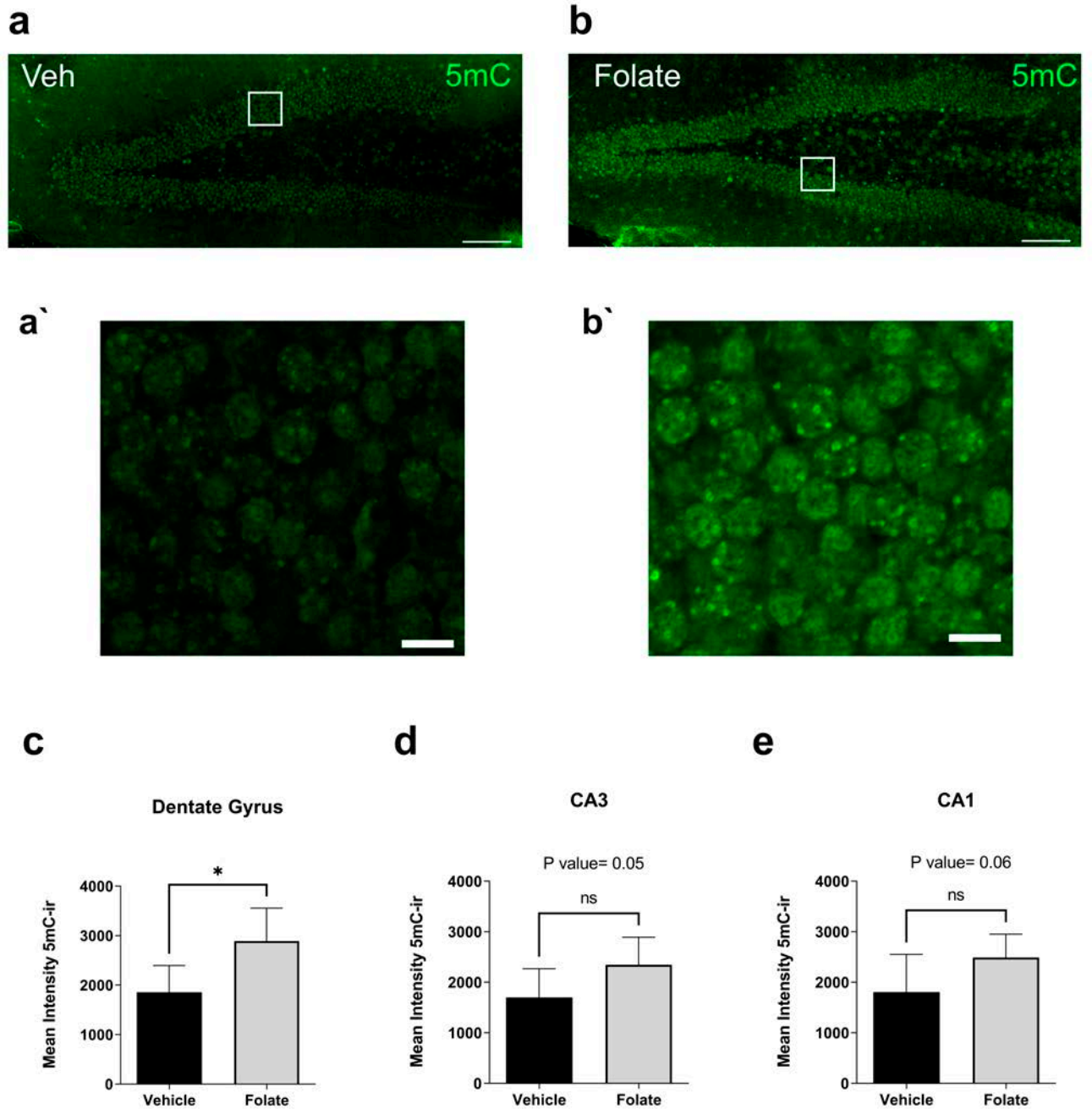
a
Veh
5mC
b
Folate
5mC
a`
b`
c
Dentate Gyrus
*
Mean Intensity 5mC-ir
4000
3000
2000
1000
0
Vehicle
Folate
d
CA3
P value= 0.05
ns
Mean Intensity 5mC-ir
4000
3000
2000
1000
0
Vehicle
Folate
e
CA1
P value= 0.06
ns
Mean Intensity 5mC-ir
4000
3000
2000
1000
0
Vehicle
Folate

Fig.3

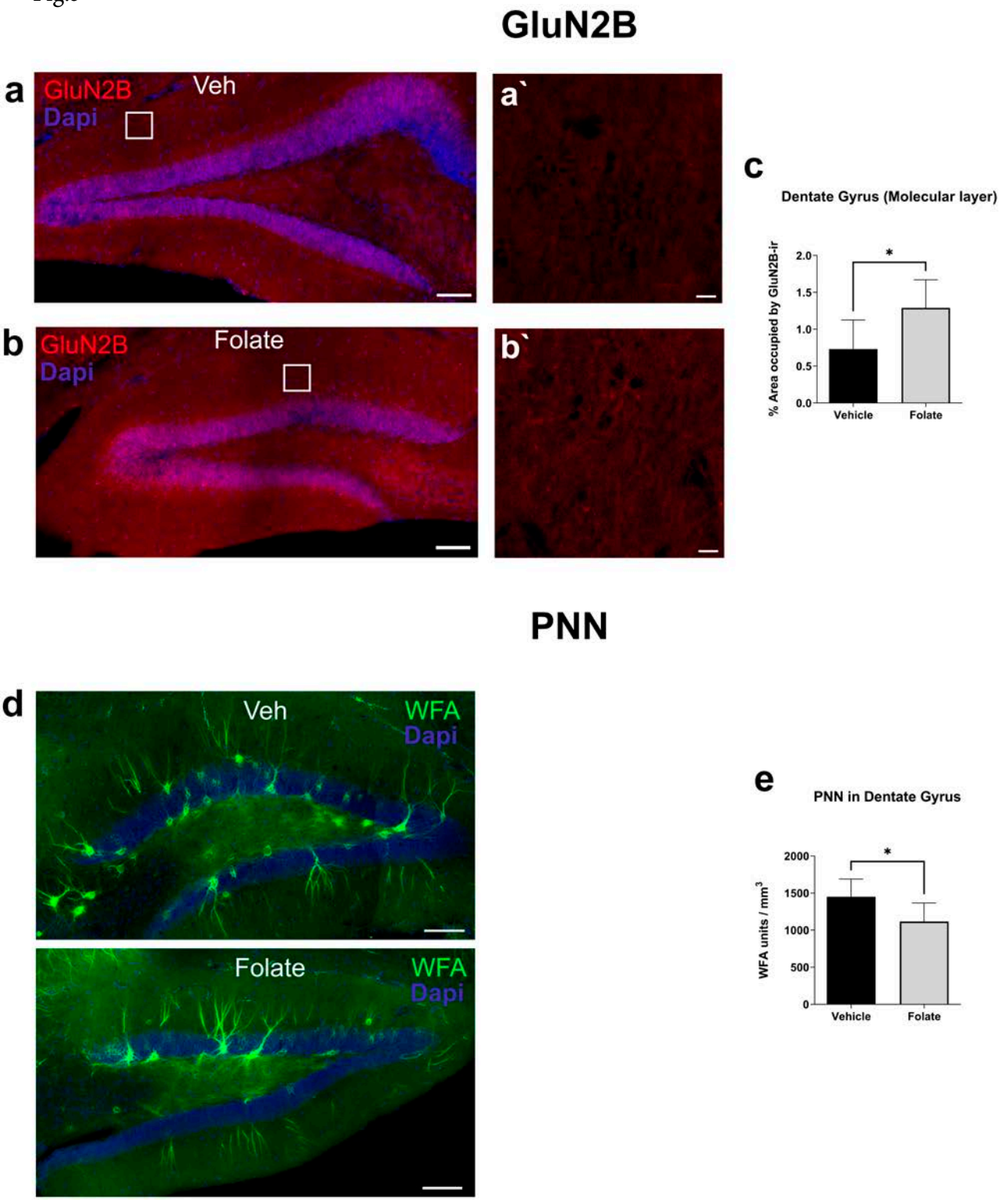
GluN2B
a
GluN2B
Dapi
Veh
a`
b
GluN2B
Dapi
Folate
b`
c
Dentate Gyrus (Molecular layer)
% Area occupied by GluN2B-ir
2.0
1.5
1.0
0.5
0.0
*
Vehicle
Folate
PNN
d
Veh
WFA
Dapi
Folate
WFA
Dapi
e
PNN in Dentate Gyrus
WFA units / mm3
2000
1500
1000
500
0
*
Vehicle
Folate

Fig.4

a

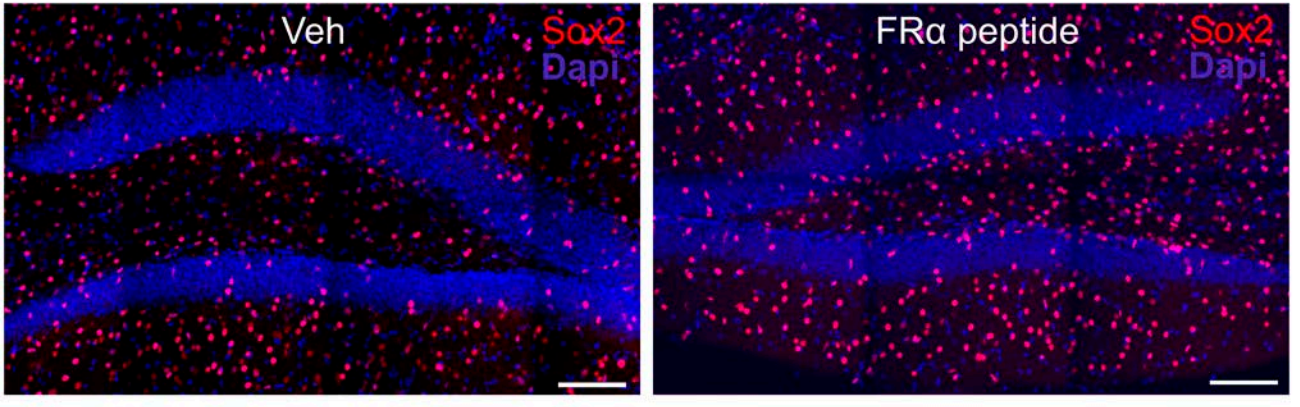
Veh
Sox2
Dapi
FRα peptide
Sox2
Dapi

b

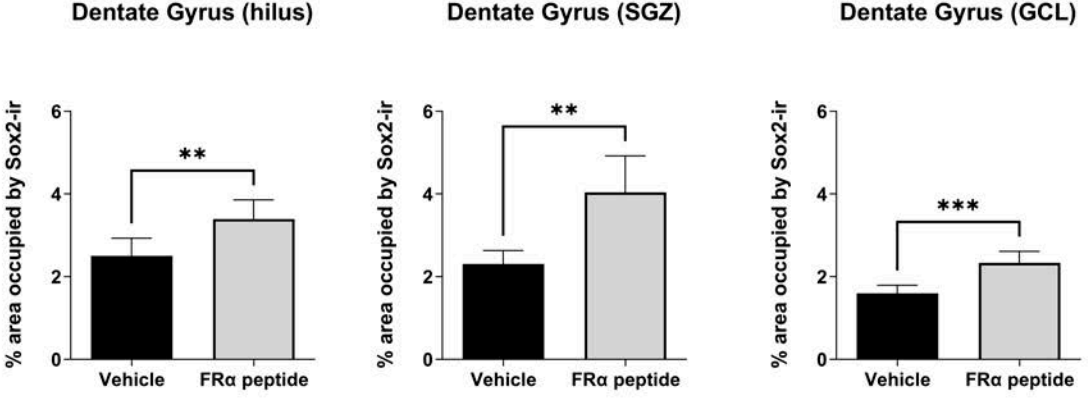
Dentate Gyrus (hilus)
Dentate Gyrus (SGZ)
Dentate Gyrus (GCL)
% area occupied by Sox2-ir
0
2
4
6
**
**
***
Vehicle
FRα peptide

Fig.5

GluN2B

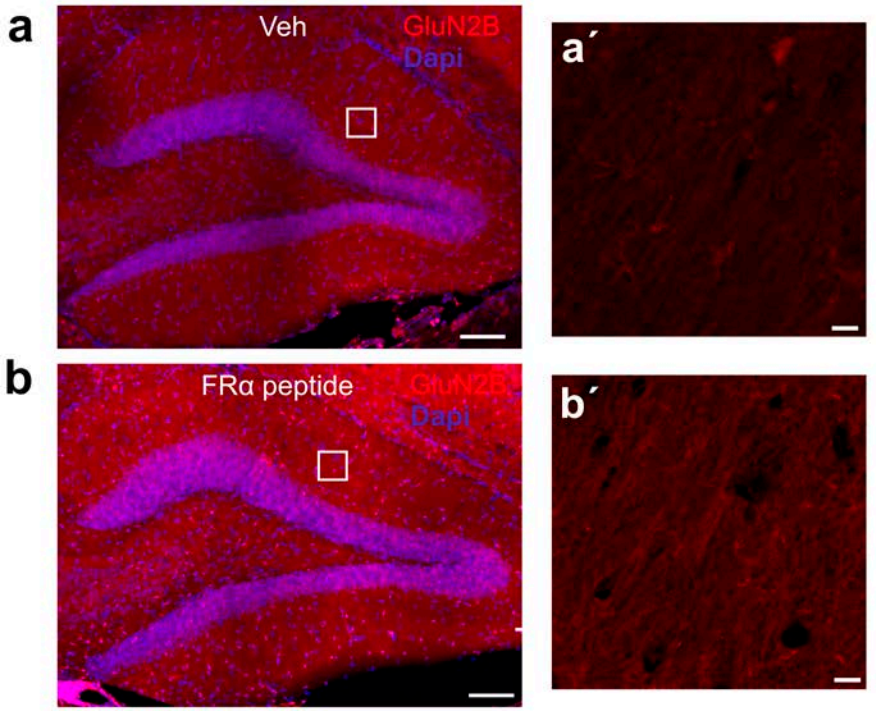

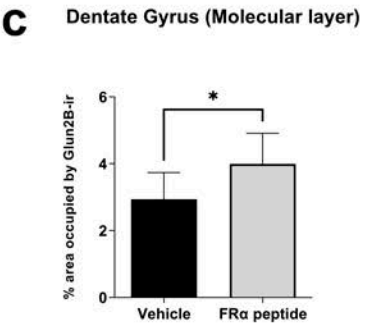

PNN

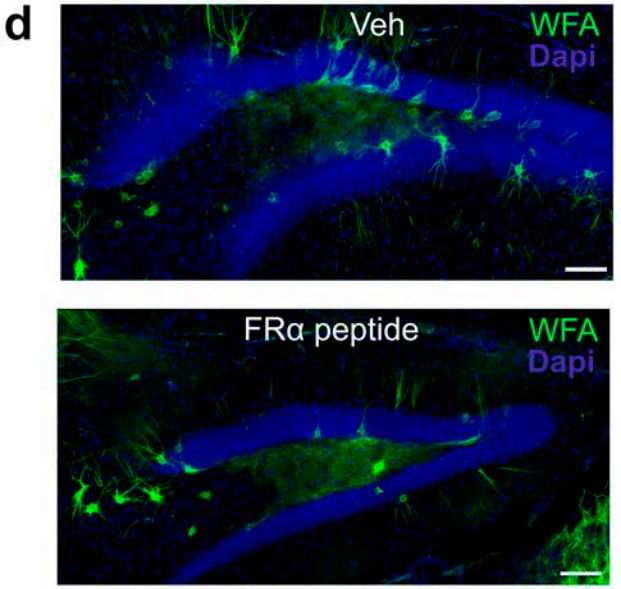

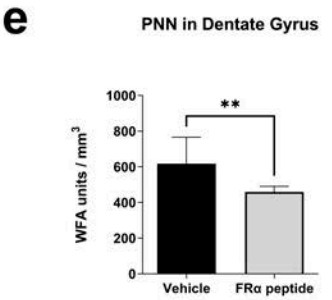

Fig.6

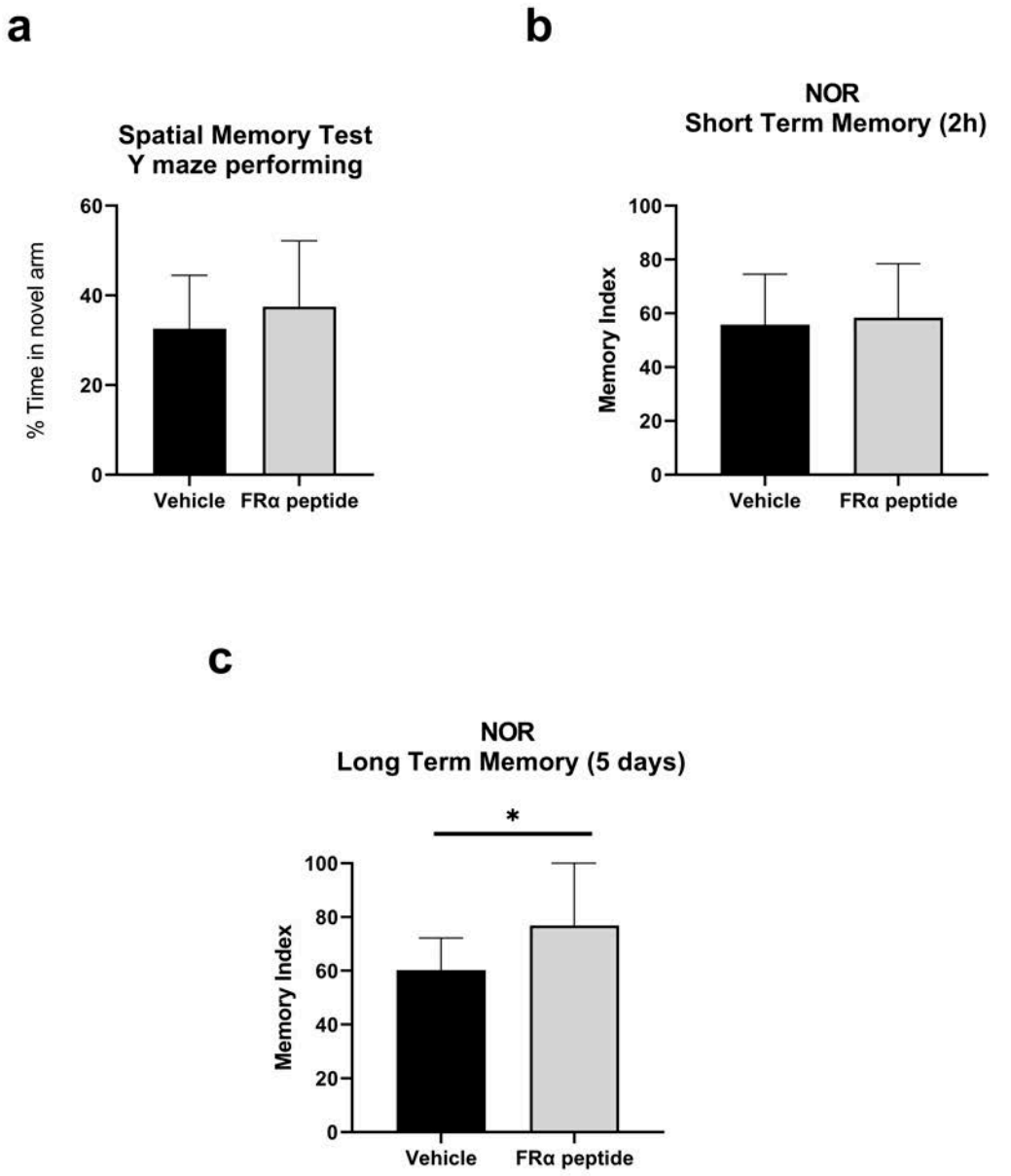
a
Spatial Memory Test
Y maze performing
% Time in novel arm
60
40
20
0
Vehicle
FRα peptide
b
NOR
Short Term Memory (2h)
Memory Index
100
80
60
40
20
0
Vehicle
FRα peptide
c
NOR
Long Term Memory (5 days)
*
Memory Index
100
80
60
40
20
0
Vehicle
FRα peptide

Fig.7

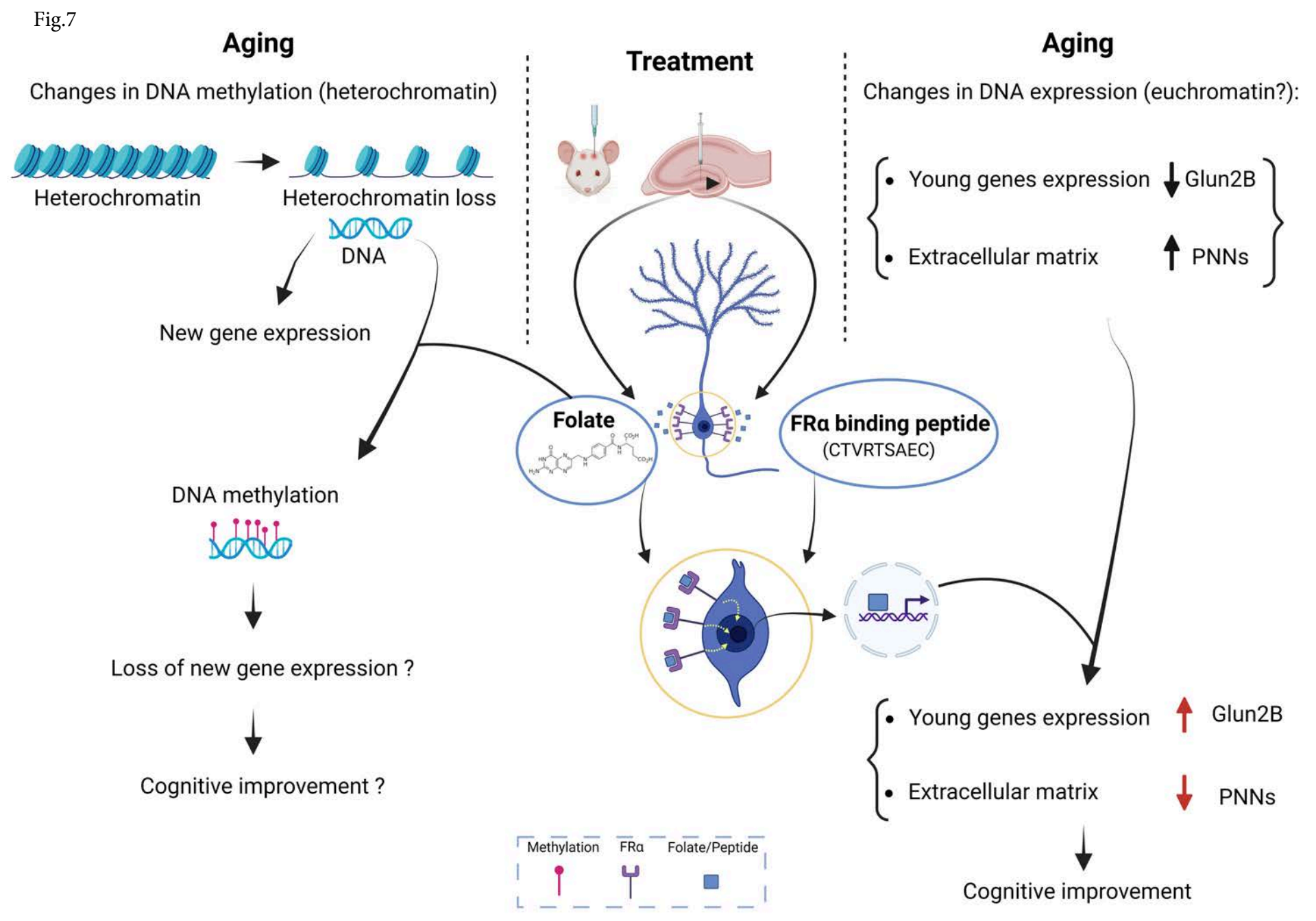
Aging
Changes in DNA methylation (heterochromatin)
Heterochromatin
Heterochromatin loss
DNA
New gene expression
DNA methylation
Loss of new gene expression ?
Cognitive improvement ?
Treatment
Folate
FRα binding peptide
(CTVRTSAEC)
Aging
Changes in DNA expression (euchromatin?):
Young genes expression
Glun2B
Extracellular matrix
PNNs
Young genes expression
Glun2B
Extracellular matrix
PNNs
Cognitive improvement
Methylation
FRα
Folate/Peptide